

ON THE PHYSICAL INTERPRETATION OF PROPER ORTHOGONAL MODES IN VIBRATIONS

B. F. FEENY

*Michigan State University
Department of Mechanical Engineering
2555 Engineering Building
East Lansing, MI 48824 USA*

R. KAPPAGANTU

*Altair Engineering, Inc.
1755 Fairlane Dr.
Allen Park, MI 48101*

Abstract

We relate the proper orthogonal modes, as applied in discrete vibration systems, to normal modes of vibration in systems with a known mass matrix. In the case of undamped free vibration, the proper orthogonal modes converge to the linear normal modes as the amount of data increases. This interpretation is also practical for lightly modally damped systems. Forced resonances lead to proper orthogonal modes which approximate vibration modes. We look at a particular case of nonlinear normal modes in which the motion of a single mode follows a curve in the coordinate space. In this case, the proper orthogonal modes represent the principal axes of inertia formed by the distribution of data on the modal coordinate curve. More generally, the proper orthogonal modes represent the principal axes of inertia of the data.

1. INTRODUCTION TO PROPER ORTHOGONAL DECOMPOSITION

The goal of this paper is to examine the relationship between proper orthogonal modes, which are explained below, and normal modes of vibration. The focus includes linear modes of vibration and a certain class of nonlinear normal modes.

The proper orthogonal decomposition (POD), also known as Karhunen-Loève decomposition, is emerging as a useful experimental tool in dynamics and vibration. Lumley [1] traced the idea back to independent investigations by Kosambi (1943), Loève (1945), Karhunen (1946), Pougachev (1953), and Obukhov (1954). It is primarily a statistical formulation, although it facilitates modal projections of partial differential equations into reduced-order deterministic models.

While the method was first applied to turbulence by Lumley in 1967 [2], it had not caught the attention of structural dynamicists until very recently. The method quantifies spatial coherence in an oscillating system with several sensors. In this sense, POD has been useful in uncovering spatial coherence in turbulence [1, 2, 3] and structures [4, 5], and determining the number of active state variables in a system [3, 4, 5]. Proper orthogonal modes (POMs) have been treated as empirical modal bases for discretizing partial differential equations by

Galerkin projection in turbulence applications [3] and more recently in structural dynamics [6, 7, 8].

Up to now, the POMs have been interpreted mainly as empirical system modes. In the analysis of turbulence, the POMs have been shown to represent the optimal distributions of kinetic energy or power, and the proper orthogonal values (POVs) indicate the power associated with these principal distributions [3, 5].

Application of POD to structures typically requires the sensed displacements of a dynamical system at M locations. We call these displacements $x_1(t), x_2(t), \dots, x_M(t)$. When the displacements are sampled N times, we can form displacement-history arrays, such that $\mathbf{x}_i = (x_i(t_1), x_i(t_2), \dots, x_i(t_N))^T$, for $i = 1 \dots M$. The means are often subtracted from the displacement histories. In performing the proper orthogonal decomposition, these displacement histories are used to form an $N \times M$ ensemble matrix,

$$\mathbf{X} = [\mathbf{x}_1, \mathbf{x}_2, \dots, \mathbf{x}_M].$$

Each row of \mathbf{X} represents a point in the coordinate space at a particular instant in time. The $M \times M$ correlation matrix $\mathbf{R} = \frac{1}{N} \mathbf{X}^T \mathbf{X}$ is then formed. Since \mathbf{R} is real and symmetric, its eigenvectors form an orthogonal basis. The eigenvectors of \mathbf{R} are the proper orthogonal modes, and the eigenvalues are the proper orthogonal values.

In this paper we point out how the POMs, formulated in this way, are related to linear and nonlinear modes of vibration.

2. LINEAR VIBRATION MODES

In this section, we consider undamped free vibrations, and then comment on modally damped and generally damped free vibrations, and also on forced vibrations.

2.1. UNDAMPED SYSTEMS

The equations of motion of an unforced, undamped linear multi-degree-of-freedom vibration system are written as

$$\mathbf{M}\ddot{\mathbf{x}} + \mathbf{K}\mathbf{x} = \mathbf{0}. \quad (1)$$

For a large class of structures, \mathbf{M} and \mathbf{K} are symmetric and positive definite. The modal vectors \mathbf{v} , when normalized with respect to the mass matrix, satisfy the orthogonality condition $\mathbf{v}_i^T \mathbf{M} \mathbf{v}_j = \delta_{ij}$. A coordinate transformation $\mathbf{x} = \mathbf{M}^{-1/2} \mathbf{q}$ can be made [9]. The system can then be recast as

$$\ddot{\mathbf{q}} + \mathbf{M}^{-1/2} \mathbf{K} \mathbf{M}^{-1/2} \mathbf{q} = \mathbf{0}, \quad (2)$$

or $\ddot{\mathbf{q}} + \mathbf{A} \mathbf{q} = \mathbf{0}$. The advantages of this representation are that its matrices are still symmetric and the effective mass matrix is the identity. Thus, given a known mass matrix, the system can be recast as an equivalent symmetric system with an identity mass matrix.

With this in mind, we discuss the free vibrations of a class of problems for which the mass matrix in the differential equation of motion is the identity. The normalized modal vectors \mathbf{v}_i of such a system satisfy the orthogonality property $\mathbf{v}_i^T \mathbf{v}_j = \delta_{ij}$.

Suppose a vibration consists of several normal modes. We can express the motion as

$$\mathbf{x}(t) = A_1 \sin(\omega_1 t - \phi_1) \mathbf{v}_1 + A_2 \sin(\omega_2 t - \phi_2) \mathbf{v}_2 + \cdots + A_M \sin(\omega_M t - \phi_M) \mathbf{v}_M, \quad (3)$$

where the components of $\mathbf{x}(t)$ are the displacements of particular coordinates, \mathbf{v}_i are the modal vectors, and the constants A_i and ϕ_i depend on the initial conditions. For short, we write equation (3) as

$$\mathbf{x}(t) = e_1(t) \mathbf{v}_1 + e_2(t) \mathbf{v}_2 + \cdots + e_M(t) \mathbf{v}_M, \quad (4)$$

where the functions $e_i(t)$ represent the time modulations of the modes.

Then the ensemble matrix has the form

$$\mathbf{X} = [\mathbf{x}(t_1) \cdots \mathbf{x}(t_N)]^T = [\mathbf{e}_1 \mathbf{v}_1^T + \cdots + \mathbf{e}_M \mathbf{v}_M^T],$$

where the vectors \mathbf{e}_i are $N \times 1$ arrays of the functions $e_i(t)$ evaluated at times $t = t_1, t_2, \dots, t_N$.

We can check whether a modal vector is actually a POM by post multiplying the matrix \mathbf{R} by a modal vector. Thus,

$$\mathbf{R} \mathbf{v}_j = \frac{1}{N} \mathbf{X}^T \mathbf{X} \mathbf{v}_j = \frac{1}{N} [\mathbf{e}_1 \mathbf{v}_1^T + \cdots + \mathbf{e}_M \mathbf{v}_M^T]^T [\mathbf{e}_1 \mathbf{v}_1^T + \cdots + \mathbf{e}_M \mathbf{v}_M^T] \mathbf{v}_j.$$

The orthogonality relation $\mathbf{v}_i^T \mathbf{v}_j = \delta_{ij}$ reduces the matrix product to

$$\mathbf{R} \mathbf{v}_j = \frac{1}{N} (\mathbf{v}_1 \mathbf{e}_1^T \mathbf{e}_j + \cdots + \mathbf{v}_M \mathbf{e}_M^T \mathbf{e}_j). \quad (5)$$

As long as the frequencies of the modes are distinct, each term $\mathbf{v}_i \mathbf{e}_i^T \mathbf{e}_j / N$ will disappear as $N \rightarrow \infty$ except for the term $\mathbf{v}_j \mathbf{e}_j^T \mathbf{e}_j$ which is proportional to \mathbf{v}_j . Hence, an eigenvector of \mathbf{R} , and thus a POM, converges to a modal vector.

If the structural system is formulated such that the mass matrix is not proportional to the identity matrix, the normalized modal vectors satisfy the orthogonality relation $\mathbf{v}_i^T \mathbf{M} \mathbf{v}_j = \delta_{ij}$. We can define $\hat{\mathbf{R}} = \mathbf{R} \mathbf{M}$, which is not a customary way of staging the POD process. ($\mathbf{R} \mathbf{M}$ is not symmetric, so technically we should no longer use the term ‘‘orthogonal.’’ However, we continue to use the POD acronyms and terminology since the process remains the same.) Then, for large numbers of data, \mathbf{v}_j is a proper mode, as can be seen by post-multiplying $\hat{\mathbf{R}}$ by \mathbf{v}_j , or \mathbf{R} by $\mathbf{M} \mathbf{v}_j$, and taking a limit to again obtain a vector which is proportional to \mathbf{v}_j . Thus, if the POD were carried out on the adjusted matrix $\hat{\mathbf{R}} = \mathbf{R} \mathbf{M}$, the resulting proper modes would converge to the system eigenvectors.

2.2. A LINEAR EXAMPLE

As an example, let us consider a chain of nondimensional masses of values 2, 1, and 1 nondimensional units, connected in series from a wall through three springs of nondimensional stiffness $k = 1$. The mechanical model is shown in Figure 1. The equations of motion are $\mathbf{M} \ddot{\mathbf{x}} + \mathbf{K} \mathbf{x} = \mathbf{0}$, where the matrices have values

$$\mathbf{M} = \begin{bmatrix} 2 & 0 & 0 \\ 0 & 1 & 0 \\ 0 & 0 & 1 \end{bmatrix}$$

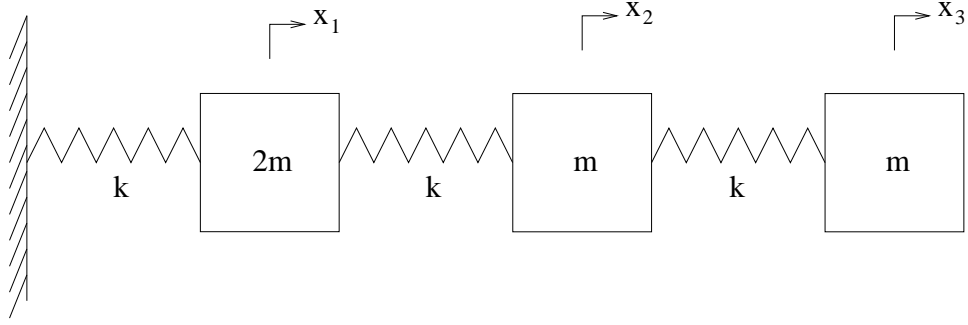


Figure 1: The mass-spring model used for the linear example has $k = 1$ and $m = 1$.

and

$$\mathbf{K} = \begin{bmatrix} 2 & -1 & 0 \\ -1 & 2 & -1 \\ 0 & -1 & 1 \end{bmatrix}.$$

This system has modal vectors

$$\hat{\mathbf{v}}_1 = (0.3602, 0.5928, 0.7204)^T,$$

$$\hat{\mathbf{v}}_2 = (0.7071, 0, -0.7071)^T,$$

and

$$\hat{\mathbf{v}}_3 = (0.2338, -0.8524, 0.4676)^T,$$

as computed by Matlab, which are orthogonal with respect to the mass matrix. Matlab does not normalize the vectors with respect to the mass matrix, rather it gives all eigenvectors a Euclidean norm of one. We leave them in the Matlab-normalized form so they can be compared directly with POMs which are also computed by Matlab. The corresponding natural frequencies are $\omega_1 = 0.4209$, $\omega_2 = 1.0000$, and $\omega_3 = 1.6801$.

The natural coordinates, or modal coordinates, are defined by a transformation of variables such that $\mathbf{x} = \mathbf{V}\mathbf{e}$, where $\mathbf{V} = [\mathbf{v}_1, \mathbf{v}_2, \mathbf{v}_3]$, and the vectors \mathbf{v}_i are normalized with respect to the mass matrix. If the initial displacements are $\mathbf{x}(0) = (1, 0, 0)^T$ and the initial velocities are zero, then the initial displacements in the natural coordinate system are

$$\mathbf{e}(0) = \mathbf{V}^T \mathbf{M} \mathbf{x}(0) = (0.6777, 1.1547, 0.4554)^T,$$

and the modal response is $\mathbf{e}(t) = (0.6777 \cos \omega_1 t, 1.1547 \cos \omega_2 t, 0.4554 \cos \omega_3 t)^T$. The response in the original coordinate system is $\mathbf{x}(t) = \mathbf{V}\mathbf{e}(t)$. We sampled this response with a sampling rate h , and computed the matrix \mathbf{R} . The eigenvectors of $\mathbf{R}\mathbf{M}$ should then be similar to the modal vectors \mathbf{v}_j . (Alternatively, we could apply the transformation $\mathbf{q} = \mathbf{M}^{1/2} \mathbf{x}$ and use the eigenvectors from the correlation matrix based on the data in \mathbf{q} .)

We computed POMs for various numbers of data obtained with various sampling rates. In one test we used $N = 200$ samples and a step size of $h = 0.1493$ nondimensional time units (two fundamental periods), and obtained POMs of $\mathbf{u}_1^T = (0.4107, 0.5898, 0.6953)^T$,

$\mathbf{u}_2^T = (0.6714, -0.0645, -0.7383)^T$, and $\mathbf{u}_3^T = (-0.2171, 0.8558, -0.4695)^T$, with corresponding POVs of $\lambda_1 = 0.2288$, $\lambda_2 = 0.6686$, and $\lambda_3 = 0.1038$. Comparing the POMs to the Matlab-normalized eigenvectors \mathbf{v}_i , and adjusting for sign changes, the mean of the norms of the errors was 0.0513. In the second test, for $N = 200$ samples, and a step size of $h = 0.2986$ nondimensional time units (four fundamental periods), we obtained POMs of $\mathbf{u}_1^T = (0.3628, 0.5870, 0.7238)^T$, $\mathbf{u}_2^T = (0.7078, -0.0037, -0.7064)^T$, and $\mathbf{u}_3^T = (-0.2293, 0.8556, -0.4641)^T$, with corresponding POVs of $\lambda_1 = 0.2308$, $\lambda_2 = 0.6703$, and $\lambda_3 = 0.1040$. The mean error norm was 0.0059. In the third test, for $N = 400$ samples, and a step size of $h = 0.1493$ nondimensional time units (four fundamental periods), we obtained POMs of $\mathbf{u}_1^T = (0.3611, 0.5921, 0.7204)^T$, $\mathbf{u}_2^T = (0.7078, -0.0038, -0.7064)^T$, and $\mathbf{u}_3^T = (-0.2315, 0.8526, -0.4685)^T$, with corresponding POVs of $\lambda_1 = 0.2302$, $\lambda_2 = 0.6786$, and $\lambda_3 = 0.1037$. The mean error norm was 0.0025.

The tests indicate that the POMs agree with the system eigenvectors. In this case, the error decreases with increasing numbers of samples, and with increasing time-record length.

Furthermore, the POVs vary with the amplitudes of the modal coordinates, which are given by the elements of $\mathbf{e}(0)$. A calculation based on equation (5) shows that each POV of $\hat{\mathbf{R}}$ converges to the mean squared value of the corresponding modal coordinate times the generalized modal mass associated with the normalization of the modal coordinate. Here, the quantities $(1/2)e_i(0)^2\mathbf{v}_i^T\mathbf{M}\mathbf{v}_i = (1/2)e_i(0)^2$, for $i = 1, 2$, and 3 , have the values 0.2297, 0.6667, and 0.1037, which correspond closely to the proper values. The interpretation that the POVs represent system energies is thus respective to the signals, and not necessarily reflective of the mechanical contribution of stiffness, frequency or velocity. We address this interpretation in Section 3.

Among the many examples which we have tried, we have encountered an example which yielded poor results. The reason will be made clear, and will be discussed in Section 5.

2.3. COMMENTS ON DAMPED SYSTEMS

For the case of damped systems, we may run into difficulty applying the ideas above, since they require that the $\lim_{N \rightarrow \infty} \mathbf{e}_i^T \mathbf{e}_j / N = 0$, for $i \neq j$, and $\lim_{N \rightarrow \infty} \mathbf{e}_i^T \mathbf{e}_i / N \neq 0$, and for damped free vibrations, the functions $e_i(t) \rightarrow 0$ themselves as $t \rightarrow \infty$. However, N is finite in practice, so we might have some luck if the modal damping factors are low enough that several cycles of vibration may be observed.

For the case of modal damping, where the modes are synchronous and real, the above results are applicable in some practical cases. As a free-vibration example, we applied modal damping to the linear example above, with $N = 400$ samples and $h = 0.1493$ (four fundamental periods). When modal damping factors of $\zeta = 0.1, 0.05$, and 0.01 were applied to each mode in three separate simulations, the mean of the norm of the errors between the resulting POMs and the natural modes were 0.1126, 0.0351, and 0.0036, respectively. Intuitively, as the modal damping decreases, the modal oscillations are sustained longer, and results improve.

For the case of general damping, one might consider a correlation matrix built out of ensembles of not just displacements but velocities also [10, 11]. This has not been the usual

way of applying POMs in structural dynamics, although there is nothing stopping us as long as the measurements are available. The normal modes are planes in the state space. We have not looked at how the POMs might span the normal-modal planes.

2.4. COMMENTS ON FORCED VIBRATION

In the case of steady-state harmonically forced vibrations, equation (5) will still hold. However, each of the time modulation terms $e_i(t)$ will have the same frequency. Therefore, none of the limits $\lim_{N \rightarrow \infty} \mathbf{e}_i^T \mathbf{e}_j / N$ are zero. We can no longer say that the POMs are convergent to the modal vectors \mathbf{v}_i .

Nonetheless, if we were to have one of the modes in resonance, such that one of the $e_i(t)$ had a much larger amplitude than the others, then the POM associated with the largest POV would approximate the resonating mode shape. The quality of the approximation would depend on the relative amplitude of the resonant modal response with respect to the nonresonating modal responses. The nonresonating mode shapes would not be detectable by the POD. If a single mode \mathbf{v}_i were active, such that $\mathbf{R} = 1/N \mathbf{v}_i \mathbf{e}_i^T \mathbf{e}_i \mathbf{v}_i^T$, then that mode would be an eigenvalue of \mathbf{R} , and hence a proper orthogonal mode, regardless of the mass distribution.

As an example, we applied a sinusoidal force to the first mass in the linear example. In such case, the relative forcing vector on the mass-normalized modal coordinates is $(0.3389, 0.5774, 0.2277)^T$. Each resonance was reached separately by setting the frequency of the excitation to the value of $\omega = \omega_i \sqrt{1 - 2\zeta^2}$. Four cycles of steady-state vibration were sampled such that 400 samples were made. The norm of the difference between the dominant POM and the resonant modal vector was calculated for each resonance case. For the case of $\zeta = 0.01$ for each resonated mode, the norms of the errors were 8.7×10^{-5} , 2.6×10^{-4} , and 1.9×10^{-4} , for the first, second, and third resonances. The ratios between the two largest POVs were 18410, 4522, and 140.0. For the case of $\zeta = 0.05$ for each mode, the norms of the residuals were 0.0022, 0.0066, and 0.0049, for the first, second, and third resonances. The ratios between the two largest POVs were 745.3, 181.0, and 5.574. For the case of $\zeta = 0.1$ for each mode, the norms of the errors were 0.0086, 0.0263, and 0.0318, for the first, second, and third resonances. The ratios between the two largest POVs were 193.3, 45.29, and 1.374.

The accuracy of these test results depends in part on the relative forcing produced on the modal coordinates, the quality of resonance, and the frequency ratios in the modal resonance curves. As ζ decreases, the modal resonance quality increases, and the results improve. The ratio between the two largest POVs hint at of what kind of quality can be expected, since the results converge as this ratio becomes very large.

3. GEOMETRIC INTERPRETATION OF THE POMS

This discussion parallels the interpretation of the singular systems analysis of a phase-space reconstruction [13]. If we consider $N\mathbf{R} = \mathbf{X}^T \mathbf{X}$, then the normalized eigenvectors \mathbf{v} of \mathbf{R} satisfy

$$\mathbf{X}^T \mathbf{X} \mathbf{v} = N \lambda \mathbf{v}.$$

We premultiply the above equation by \mathbf{v}^T to obtain $\mathbf{v}^T \mathbf{X}^T \mathbf{X} \mathbf{v} = N\lambda$. Let us take a closer look at $\mathbf{X} \mathbf{v}$. Since \mathbf{X} consists of columns of sampled data from each coordinate, the rows of \mathbf{X} represent coordinate points at each instant in time. We label these coordinate points \mathbf{p}_j , such that the rows of \mathbf{X} are given by \mathbf{p}_j^T . Thus we have

$$\mathbf{X} \mathbf{v} = [\mathbf{v}^T \mathbf{p}_1, \mathbf{v}^T \mathbf{p}_2, \dots, \mathbf{v}^T \mathbf{p}_N]^T.$$

Each element of the vector $\mathbf{X} \mathbf{v}$ consists of the projection of each coordinate point \mathbf{p}_j onto the unit vector \mathbf{v} , giving its distance along the direction of \mathbf{v} from the origin. Thus, the quantity $\frac{1}{N} \mathbf{v}^T \mathbf{X}^T \mathbf{X} \mathbf{v} = \frac{1}{N} (\mathbf{X} \mathbf{v})^T \mathbf{X} \mathbf{v} = \lambda$ equals the mean squared distance of coordinate data projected along the axis of \mathbf{v} . The eigenvectors, or proper orthogonal modes, then optimize the mean squared distances of data along an orthogonal basis. In mechanical systems, distances squared are associated with energy. In fluids, velocities are measured, and the mean squared values would be associated with kinetic energy. Hence we have an interpretation consistent with the known property that the POMs indicate the optimal energy or power distributions in the data [3].

Furthermore, it turns out that the POMs coincide with the principle axes of the ellipsoid of inertia formed by this “mass” distribution. To see this, let us revisit the correlation matrix built from M sensor displacements, x_i . We label each sample as x_{ij} , where $j = 1, \dots, N$ are the time indices. The elements of the correlation matrix then have the form

$$R_{ik} = \frac{1}{N} \sum_{j=1}^N x_{ij} x_{kj}.$$

If each data has unit mass, then $N\mathbf{R}$ is related to the matrix representation of the M th-order moment-of-inertia tensor \mathbf{J} by $N\mathbf{R} = \rho \mathbf{I}_M - \mathbf{J}$, where $\rho = \sum_{j=1}^N \sum_{i=1}^M x_{ij}^2$ is the sum of distances of the data from the origin, and \mathbf{I}_M is the $M \times M$ identity matrix. Incidentally, $\rho = \text{trace}(N\mathbf{R}) = \sum_{i=1}^M N\lambda_i$. The eigenvalues of \mathbf{J} indicate the principal moments of inertia $\alpha_i \geq 0$, and the eigenvectors of \mathbf{J} satisfy $\mathbf{J}\phi = \alpha\phi$. Then

$$N\mathbf{R}\phi = \rho \mathbf{I}_M \phi - \mathbf{J}\phi = \rho\phi - \alpha\phi = (\rho - \alpha)\phi.$$

Therefore the principal axes of inertia are eigenvectors of \mathbf{R} and thus coincide with the POMs. Furthermore, the POVs are related to the principal moments of inertia by $N\lambda_i = \rho - \alpha_i$, for $i = 1, \dots, M$. This means that the axis corresponding to the largest proper orthogonal value, which is associated with the largest mean projected distance of data, corresponds to the axis about which we have the smallest moment of inertia.

4. NONLINEAR MODES

A nonlinear normal mode can be viewed as an invariant manifold in the state-space description of a system [12]. Proper orthogonal decomposition, as formulated here, is employed on measurements of the displacement coordinates, rather than measurements of full states. (However, as mentioned above, in some cases POD has been applied to full state-variable measurements, as long as it is possible to obtain them.) For this discussion, we consider

the situation for which the motion is of a single, pure, synchronous nonlinear mode. By “synchronous” we mean that all displacement coordinates reach their extreme values simultaneously. We also assume that the dynamics on the invariant manifold, when projected onto the coordinate space, does not show any hysteretic behavior in the coordinate space during motions.

In such case, the data accumulates on a nonlinear curve in the coordinate space. The POMs are thus the principal axes of inertia of these data as if they were points on a scaffold defined by the nonlinear modal curve. The principal axes of an ellipsoid of inertia optimize the squares of the distances of the particles to the axes. Thus, the POMs could be viewed in the least-squares sense as an optimization of the “error” in the choice of a linear representation of the nonlinear normal mode, under the constraint that the linear representation goes through the origin of the coordinate system. This differs from the typical application of least squares in that the optimized distances associated with the POMs are perpendicular distances, rather than errors defined through one of the coordinates only (as in fitting a curve $y = mx$ to (x_i, y_i) data, for which the errors $y - y_i$ are minimized). The proper orthogonal values, as do the relative magnitudes of the principal moments of inertia, hint at how much the data deviates from the linear approximations suggested by the POMs. The POMs depend on the invariant manifold, and on how the data populates the manifold.

If the motion is on a higher-dimensional invariant manifold, for example if more than one synchronous nonlinear modes are active, or if the nonlinear normal mode is not synchronous, then the POMs would again represent principal axes of the ellipsoid of inertia associated with the sampled data. However, the relationship between the POMs and the “best fit” of the nonlinear normal modes is obscured.

Berkooz *et al.* [3] commented that although the proper orthogonal decomposition is a linear process, it “may not do the physical violence of linearization methods”. Indeed, if one were to project the differential equations onto the dominant POM, as in our two-degree-of-freedom example, the gist of the nonlinearity would be preserved in that projection, which merely follows, in an optimal way, the modal contour.

4.1. A NONLINEAR EXAMPLE

We show an example of two unit masses which are spring connected between two walls (Figure 1). The first mass is connected to a wall through a nonlinear spring which behaves according to $F_{nl} = x^3$. The other mass is connected to the other wall through a linear spring of unit stiffness. The coupling spring between the two masses also has unit stiffness. The equations of motion are

$$\ddot{x}_1 + x_1 - x_2 + x_1^3 = 0, \tag{6}$$

$$\ddot{x}_2 - x_1 + 2x_2 = 0. \tag{7}$$

The nonlinear normal modes in this system were analyzed by Shaw and Pierre [12] for small motion. We have simulated a large nonlinear normal-mode motion, and plotted x_2 versus x_1 during the oscillation, as shown in Figure 3. The displacements are confined to a curve, indicating synchronicity in the sense that x_1 and x_2 reach their maxima and

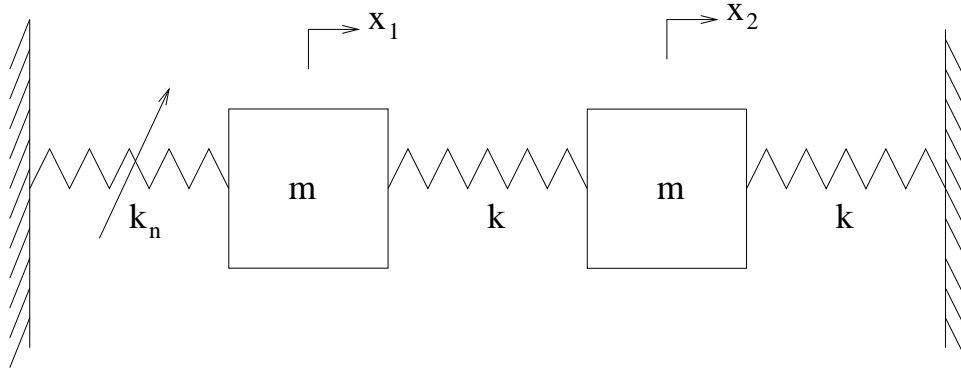


Figure 2: The model of a system with a nonlinear normal mode. We use $m = k = 1$. k_n represents a nonlinear spring through which the force is x^3 .

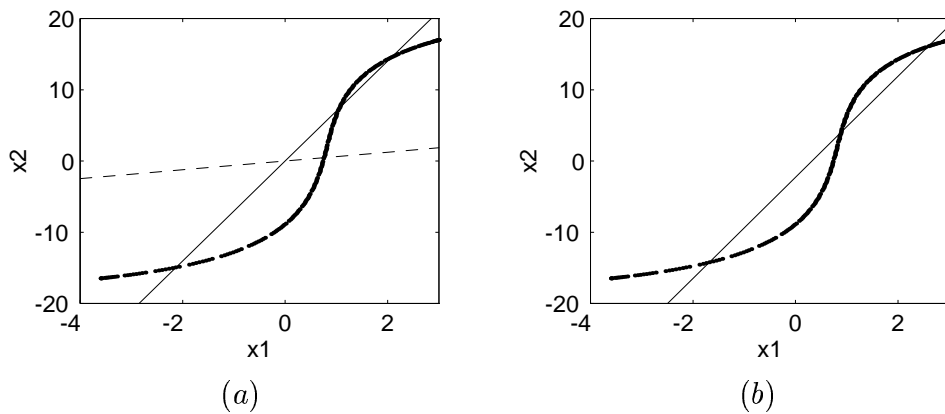


Figure 3: “Synchronous” motion data for a nonlinear two-mass system. The straight solid line represents the orientation of the dominant proper orthogonal mode based (a) at the origin, and (b) at the mean of the data. The dashed line in (a) depicts the first mode of the linearized system.

minima simultaneously. The POM associated with the most “power”, calculated from 200 data representing about four periods of oscillation, is plotted as a solid line along with the (x_1, x_2) data. This is shown in Figure 3(a) for data which is not mean adjusted. Thus, this POM indicates the axis of the smallest moment of inertia, and the largest mean squared projection, based at the origin. The first normal mode (the only mode in which the masses are moving in phase) of the linearized system is plotted as a dashed line to emphasize its deviation from the POM and the associated large-amplitude nonlinear normal mode. The POM shown in Figure 3(b) was computed for data for which the mean was subtracted. Thus, the POM represents the principal axis of inertia based at the mean of the data in the plot.

5. NUMERICAL ANOMALIES

If the data forms an ellipsoid of inertia for which two of the principal moments of inertia are the same, the representation of the associated axes of inertia is not uniquely defined. This can cause problems in determining the true modal vectors.

In Section 2.2, we mentioned that we had encountered an example which produced poor results. In that example, the set-up was similar to that of Figure 1, except that the masses were uniform so that the mass matrix was the identity, and the third mass was attached to a second wall with a fourth spring, such that the stiffness matrix was

$$\mathbf{K} = \begin{bmatrix} 2 & -1 & 0 \\ -1 & 2 & -1 \\ 0 & -1 & 2 \end{bmatrix}.$$

The initial conditions were $\mathbf{x}_0 = (1, 0, 0)^T$. Two of the eigenvalues of the correlation matrix \mathbf{R} , as obtained from Matlab, differed substantially from the system modes. However, when the modes were multiplied into the correlation matrix, such as $\mathbf{R}\mathbf{v}_j$, the result was “nearly” parallel to \mathbf{v}_j .

It turns out that the initial conditions were such that two of the modal coordinates had the same amplitude of vibration, and the ellipsoid of inertia represented by the distribution of the solution curves in the displacement-coordinate space had two equal principal moments of inertia. Indeed, the proper orthogonal values for that example, with $N = 400$ samples and $h = 0.1493$, were 0.1233, 0.2505, and 0.1274. The POVs 0.1233 and 0.1274 are finite-data approximations of identical values for which the axes of inertia, and hence the proper orthogonal modes, would not be uniquely defined. However, the true modal vectors would still represent a choice of proper orthogonal vectors. Although the POVs showed slight deviation, Matlab computed a set of POMs which differed from the modal vectors. Still, the modal vectors very nearly satisfied $\mathbf{R}\mathbf{v} = \lambda\mathbf{v}$.

The occurrence of this situation can be detected simply by checking for nearly repeated proper orthogonal values.

6. CONCLUSION

We have sketched some relationships between the proper orthogonal modes and modes of vibration. This compliments existing statistical interpretations of POMs with physical and geometric interpretations.

For the linear undamped free-vibration case formulated as a symmetric system with an identity mass matrix, the POMs represent the linear modes of vibration. This is also true for modally damped linear systems. Since the POD is so simple to implement, perhaps it will replace traditional modal analysis in some experimental applications. However, in order to describe mode shapes in the displacement coordinates, the mass matrix must be known.

The principal axes of the distribution of data coincide with the POMs. The POVs indicate the mean squared projections of the data onto these axes, and are related to the principal moments of inertia about axes based at the origin of the coordinate system, which

are the sums of the squares of the distances of data from the principal axes. Thus, for the case of a “synchronous” nonlinear normal mode, the dominant POM represents an optimal fit of a linear mode to the data on the nonlinear normal mode in the sense that the distances of data from the POM axis are optimized.

We tested our results on low-dimensional numerical examples. Further work might examine the robustness of these ideas as the numbers of degrees of freedom get large, and as noise is introduced to the data. Other future work might address the recovery of traveling wave modes, or their out-of-phase components, in systems with generalized damping. Also, studies might focus on POD for systems which have full state measurements, and deal with implications regarding the recovery of generalized modes in the state-space, as in the estimation of higher-dimensional invariant manifolds in nonlinear systems.

7. ACKNOWLEDGEMENTS

This work was supported in part by NSF grant number 9624347. We thank Steve Shaw and Gábor Stépán for discussions.

8. REFERENCES

1. J. L. Lumley 1970 *Stochastic Tools in Turbulence*, Academic Press, New York.
2. J. L. Lumley 1967 *Atmospheric Turbulence and Radio Wave Propagation*, A. M Yaglom and V. I. Tatarski, eds., Nauka, Moscow, 166-178. The structure of inhomogeneous turbulent flow.
3. G. Berkooz, P. Holmes, and J. L. Lumley 1993 *Annual Review of Fluid Mechanics* **25** 539-575. The proper orthogonal decomposition in the analysis of turbulent flows.
4. J. P. Cusumano and B.-Y. Bai 1993 *Chaos, Solitons, and Fractals* **3** (5) 515-535. Period-infinity periodic motions, chaos, and spatial coherence in a 10 degree of freedom impact oscillator.
5. J. P. Cusumano, M. T. Sharkady, and B. W. Kimble 1993 *Aerospace Structures: Non-linear Dynamics and System Response*, ASME AD-Vol. 33, 13-22. Spatial coherence measurements of a chaotic flexible-beam impact oscillator.
6. P. FitzSimons, and C. Rui 1993 *Advances in Robust and Nonlinear Control Systems*, ASME DSC-Vol. 53. Determining low dimensional models of distributed systems.
7. K. Murphy 1996 *Sixth conference on Nonlinear Vibrations, Stability, and Dynamics of Structures*, Blacksburg, VA. Using the Karhunen-Loève decomposition to examine chaotic snap-through oscillations of a buckled plate.
8. S. R. Sipicic, A. Bengeudouar, and A. Pecore 1996 *Sixth conference on Nonlinear Vibrations, Stability, and Dynamics of Structures*, Blacksburg, VA. Karhunen-Loève decomposition in dynamical modeling.
9. D. Inman 1994 *Engineering Vibration*, Prentice Hall, Englewood Cliffs.
10. I. T. Georgiou and I. B. Schwartz 1996 *Nonlinear Dynamics and Controls* ASME DE-Vol. 91 7-12. A proper orthogonal decomposition approach to coupled mechanical systems.

11. E. Kreuzer and O. Kust 1996 *Nonlinear Dynamics and Controls* ASME DE-Vol. 91 105-110. Proper orthogonal decomposition—an efficient means of controlling self-excited vibrations of long torsional strings.
12. S. W. Shaw and C. Pierre 1993 *Journal of Sound and Vibration* **164** (1) 85-124. Normal modes for non-linear vibratory systems.
13. D. S. Broomhead and G. P. King 1986 *Physica D* **20** 217-236. Extracting qualitative dynamics from experimental data.